Ultrathin Transparent Conductive Films of Polymer-Modified Multiwalled Carbon Nanotubes

Vera Bocharova,[†] Anton Kiriy,*[,†,§] Ulrich Oertel,[†] Manfred Stamm,[†] François Stoffelbach,[‡] Robert Jérôme,*[,‡,#] and Christophe Detrembleur[‡]

Leibniz-Institut für Polymerforschung Dresden, Hohe Strasse 6, 01069 Dresden, Germany, and Center for Education and Research on Macromolecules (CERM), University of Liege, Sart-Tilman, B6, 4000 Liege, Belgium

Received: April 21, 2006; In Final Form: June 13, 2006

Deposition of multiwalled carbon nanotubes modified by poly(2-vinylpyridine) (CNT-*g*-P2VP) from aqueous dispersions at low pH is an effective method to prepare homogeneous ultrathin films with a tunable CNTs density. A percolation threshold of 0.25 μg/cm^2 and a critical exponent $\alpha = 1.24$ have been found from dc conductivity measurements. The sheet resistance value agrees with the percolation theory for 2D films. According to AFM and electrical measurements, even when only 5% of the surface is covered by CNT-*g*-P2VPs, the sheet resistance is of the order of 1 MΩ/sq, which indicates that conductivity is imparted by a network of an ultralow density. When the film transmittance decreases down to ∼70% at 550 nm, the occupied surface area is ∼15% and sheet resistance falls down to ∼90 kΩ/sq. These data show that undesired in-plane clustering does not occur upon the dispersion casting of the films and that high-quality networks of CNT-*g*-P2VPs are built up. The electrosteric stabilization of the CNT-*g*-P2VP dispersions in water at low pH is at the origin of this desired behavior. Although the multiwalled CNT films prepared in this work are less conductive and less transparent than the SWNTs films, they could find applications, e.g., in touch screens, reflective displays, EMI shielding, and static charge dissipation.

1. Introduction

Because of outstanding mechanical, thermal, and electrical properties,[1] carbon nanotubes (CNTs) are of great interest for both industrial and fundamental research. Dispersion of CNTs within intrinsically insulating polymers is a straightforward way to make them extrinsically conductive.[2] This achievement is directly related to the percolation threshold of the CNTs, which is observed as a sharp drop in resistivity as soon as a 3-dimensional (3D) CNTs network is formed. CNTs-based nanocomposites usually exhibit a lower percolation threshold and a higher conductivity than materials loaded with other fillers because of the high intrinsic conductivity and the high aspect ratio of CNTs. CNTs have a strong tendency to aggregate rather than to disperse in common solvents and polymers, as a result of lack of favorable cross-interactions. Therefore (electro)steric barriers have to be built up around the CNTs, which is detrimental to the contacts between the nanotubes and to the conductivity of the nanocomposites even at a relatively high content of CNTs. The conductivity is then controlled by a tunneling effect through the insulating layer around the nanotubes rather than by their intrinsic conductivity.[3]

Selective localization of all the CNTs at an interface instead of a homogeneous dispersion within the whole composite volume[4] is an alternative approach to conductive materials with a low CNTs content, provided, however, that the surface (2D) conductivity is high enough.[5] This general concept was illustrated several years ago by the selective localization of carbon black particles (CB) at the interface of a co-continuous two-phase polymer blend.[6] Conductivity was observed at loadings as low as 0.4 wt % CB content. An intermediate situation between the 3D dispersion of CNTs and the 2D localization at an interface may be found in the preparation of ultrathin films of CNTs containing polymers. The CNTs dispersion is then borderline between a 2D and a 3D space. Moreover, much attention is paid nowadays to highly conductive ultrathin films and coatings for their performances in electromagnetic interference (EMI) shielding,[7] heat and static charge dissipation,[8] and field-emission sources.[9]

The key issue for the manufacture of high-quality films with optimized transparency and conductivity is the capability to disperse properly CNTs in an appropriate solvent[10] and to prevent the unfavorable in-plane clustering of CNTs upon drying. Kumar, Smaley, et al. dispersed single-wall carbon nanotubes (SWNTs) in oleum. The strong electrostatic repulsion of the protonated CNTs could prevent the CNTs from aggregating, and highly conductive films were prepared by casting.[11] The use of an extremely aggressive solvent is, however, a major drawback. Wu et al.[12] and Grüner et al.[13] proposed a technique based on the fast filtration of suspensions of SWNTs through a membrane intended to be dissolved afterward. The in-plane aggregation of the collected CNTs did not occur because of the fast release of the solvent. Rogers et al. reported on the controlled flocculation of SWNTs from surfactant-stabilized suspensions by addition of proper solvents.[14] Recently, Manohar et al. prepared 1500 nm films by the direct casting of SWNT dispersion in an aqueous solution of Triton-X 100.[5] Sheet resistance (∼80 Ω/sq), dc conductivity (∼50 S cm^{-1}), and

* Address correspondence to this author.
[†] Leibniz-Institut für Polymerforschung Dresden.
[§] E-mail: kiriy@ipfdd.de. Phone: +49-351-4658-271. Fax: +49-351-4658-284.
[‡] University of Liege.
[#] E-mail: rjerome@ulg.ac.be. Phone: +32-4-3663-565. Fax: +32-4-3663-497.

10.1021/jp062458e CCC: $33.50
Published on Web 07/11/2006

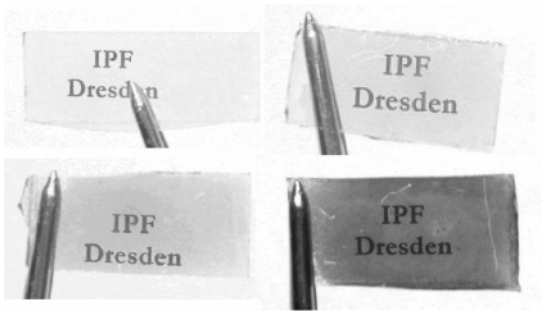

Figure 1. Pictures of CNT-*g*-P2VP films deposited on glass slides with the following transparency (T) and sheet resistance ($R\square$): (a) $T = 80\%$, $R\square = 250$ kΩ; (b) $T = 73\%$, $R\square = 120$ kΩ; (c) $T = 55\%$, $R\square = 14$ kΩ; and (d) $T = 50\%$, $R\square = 5$ kΩ.

transmittance (~80%) were measured. At the present time, all the methods proposed to prepare CNTs-based transparent conductive coatings have been tested with SWNTs and not for MWNTs.[15] The problem is that the light absorption by MWNTs is higher compared to that for SWNTs with all the other conditions being the same,[16] which makes the preparation of *transparent* conductive coatings more challenging. This paper aims at using MWNTs modified by poly(2-vinylpyridine) (P2VP)[17] for the preparation of ultrathin films and at investigating their morphology, conductivity, and transparency.

2. Results

In this work, MWNTs have been modified by a brush of P2VP of a low density and a small thickness to make them dispersible while preserving a high enough conductivity. Because the length of the chains to be grafted to the CNTs can be predetermined, the "grafting to" method has been selected.[17] The choice of P2VP has to be found in the easy ionization of the grafted chains, and thus the feasible MWNTs dispersion in water. Most of the methods of CNTs modification reported so far require the oxidative pretreatment of the surface which leads to the nanotubes shortening and thus to the increase of the percolation threshold. To avoid this drawback, the P2VP chains have been covalently grafted to MWNTs by the addition of alkoxyamine (TEMPO) end-capped P2VP.[17] By using a P2VP with a molecular weight (M_n) of 7606 g/mol, the modified MWNTs contain 13% of grafted P2VP and the thickness of this polymer shell of about 3 nm has proved to be sufficient to solubilize CNT-*g*-P2VP in "good" solvents for P2VP (~3 mg/mL), including acidified water and THF. These dispersions were used for the preparation of CNT-*g*-P2VP thin films on Si-wafers and glass slides, respectively.

Almost no deposition of carbon nanotubes is observed when an aqueous dispersion of CNT-*g*-P2VP (pH 2; ~3 mg modified MWNT/mL) is *spin-coated* onto freshly cleaned Si-wafers or glass slides. However, smooth and transparent gray films are formed upon *drop casting* of the same dispersions of CNT-*g*-P2VP, followed by solvent elimination at high temperature (150 °C) and normal pressure. The samples deposited on both cleaned Si and glass slides have been analyzed by dc electrical measurements, AFM, ellipsometry, and UV−vis spectroscopy (Figure 1 and Table 1).

TABLE 2: Transmittance at 550 nm and Sheet Resistance for CNT-*g*-P2VP Films Deposited onto Glass Slides

	entry									
	1	2	3	4	5	6	7	8	9	10
$R\square$, KΩ/sq	325	250	150	140	120	14	12.5	11	5	2.5
T, %	77	80	76	75	73	55	53	59	50	25

Samples with different nanotube surface densities, M, i.e., weight of CNT-*g*-P2VPs per cm^2, have been prepared on Si-wafers and glass slides. Assuming that the nanotubes homogeneously cover the whole surface area, the surface density of the nanotubes has been calculated as $M = V \times C/S$, where C is the weight concentration of the CNT in the dispersion of CNT-*g*-P2VP, V is the volume of the dispersion used for the film preparation, and S is the coated surface. Different spots of the surface have been probed by ellipsometry to estimate the homogeneity of the CNT-*g*-P2VP deposition. Ellipsometry was used in this work to measure the surface density of the nanotubes rather than to determine the real film thickness (the thickness was measured by atomic force microscopy, AFM, see below). An accurate measurement of the thickness of the CNT-*g*-P2VP films by ellipsometry was impossible, since the film porosity is unknown and changes from sample to sample. Using ellipsometry we measured ψ and δ angles for each film and knowing the refractive index of graphite ($n = 2.1$), we calculated the (imaginary) thickness of graphite that constitutes the nanotubes in the given film.[18] The surface density of the nanotubes (M_{el}) in each sample has been calculated from the ellipsometrically derived thickness of graphite, the density of graphite ($\rho = 2.25$ g/cm^3), and the CNTs content in the CNT-*g*-P2VP composite.[19] As a rule, the agreement is rather good between the surface densities estimated by ellipsometry (M_{el}) and calculated from the amount of deposited nanotubes, especially for thinner and more homogeneous films (M, Table 1).[20]

The resistance of CNT-*g*-P2VP films measured by a standard two-probe method depends on the deposited amount of CNT-*g*-P2VP. The reproducibility of the $I-V$ characteristics (Figure 2) together with the predictable dependence of the resistance from the film thickness and the interelectrode distance support that the experimental resistance is due to nanotube films and not the resistance of the nanotube/electrode junction. Moreover, the sheet resistance ($R\square$) is ~1 kΩ/sq.

The CNT-*g*-P2VP films have been observed by AFM, as illustrated by Figure 3 in relation to the surface density. At low M, the nanotubes are loosely packed and bare Si-surface is extensively exposed (Figure 3a). At higher M, entangled networks of nanotubes are formed (Figure 3b,c). The film thickness has been approximated by the standard AFM scratch-test (d_{AFM} in Table 1). The images for the film of the lower density (Figure 4a) have been analyzed to measure the contour

TABLE 1: Sheet Resistance for CNT-*g*-P2VP Films with Different Surface Densities, Deposited on Si-Wafers

entry	C, mg/mL	V, mL	M, μg/cm^2	d_{theor}, nm	d_{el}, nm	M_{el}, μg/cm^2	d_{AFM}, nm	$R\square$, kΩ/sq
1	0.0088	0.05	0.22	1.10	1.2	0.27	25	5000
2	0.044	0.03	0.66	3.32	4.4	0.99	50	300
3	0.177	0.01	0.88	4.42	4.9	1.1	50	90
4	0.177	0.02	1.77	8.84	6.9	1.6	70	32
5	0.177	0.03	2.65	13.27	11.8	2.7	80	20
6	0.88	0.01	4.42	22.12	17.5	3.9	100	12.5
7	0.88	0.02	9.09	44.25	19.8	4.5	120	7
8	1.77	0.05	44.24	221.2	145	32.7	700	1.3

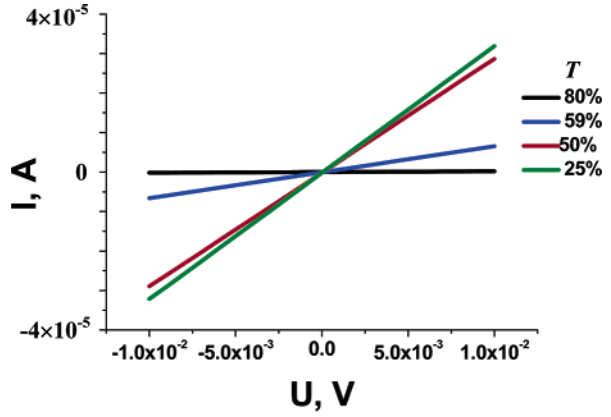

Figure 2. *I*−*V* characteristics of the CNT-*g*-P2VP films of different transparency (*T*) deposited on glass slides.

length of the individual nanotubes with dedicated software. A weight average contour length of the nanotubes (l_{AFM} = 2.4 μm, Figure 4b) has been calculated by a statistical treatment of these data. According to the classical percolation theory, this value corresponds to the length of a "conducting stick".[12,20,21] The apparent width of individual CNTs (D_{AFM}) and their occupied surface area (S_{AFM}) have also been determined with standard software,[22] l_{AFM} being the S_{AFM}/D_{AFM} ratio.

The width of the nanotubes measured by AFM is overestimated by the tip-broadening effect. For instance, a nanotube with a height (and diameter) of 25 nm is observed by AFM as a 98 nm thick object. However, this overestimation is systematic and basically constant for images recorded at the same length scale. Therefore, the statistical treatment of the data allows the overall length of nanotubes ($\sum L$) and the number density of the "conducting sticks" (N) on the image of area s to be calculated even for samples with highly entangled nanotubes:

$$\sum L = \sum S/D_{AFM};\ N = \sum L/(s \times l_{AFM})$$

The critical number density of conductive sticks (N_C)[12] at the percolation threshold has been calculated from l_{AFM}, according to

$$l\sqrt{\pi}Nc = 4.236;\ N_C = 4.236^2/(\pi \times l_{AFM}{}^2) = 17.94/(2.4^2 \times 3.14) = 0.99(1/\mu m^2)$$

The sheet resistance is higher ($R\square \sim 5$ MΩ) for sample #1 (s = 24.6 μm^2), for which the overall contour length of the nanotubes and the number density of "conducting sticks" (with the length equal to 2.4 μm) have been calculated from the AFM data. $\sum S$ and D_{AFM} are 6.15 μm^2 and 0.098 μm, respectively, as determined by the image processing:

$$\sum L = \sum S/D_{AFM} = 6.15/0.098 = 62.8;\ N_{\#1} = \sum L/(s \times l_{AFM}) = 62.8/(24.6 \times 2.4) = 1.06(1/\mu m^2)$$

Figure 5 shows that the dependence of the sheet conductance ($1/R\square$) on the surface density (M) of the CNT-*g*-P2VPs is typical of a percolative behavior. According to the percolation theory, the sheet conductance depends on the density of the conductive filler, as follows:

$$1/R\square \propto 1/R\square^0(M - M_C)^\alpha$$

where $1/R\square^0$ is the sheet conductance of the bulk material, M_C is the critical density at the percolation threshold,[23] and α is a

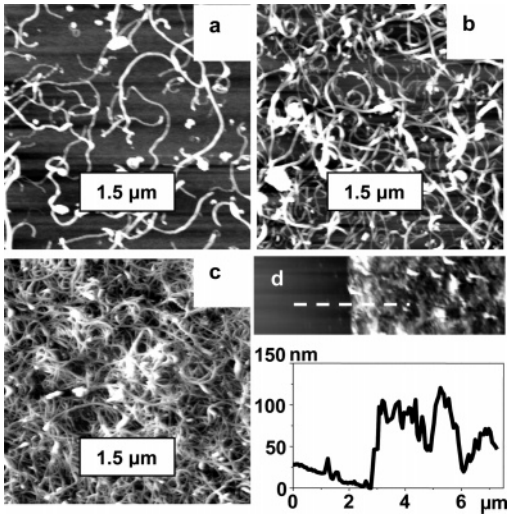

Figure 3. AFM topography images of CNT-*g*-P2VP films listed in Table 1: (a) #1, M = 0.25 μg/cm^2, R = 5 MΩ; (b) #3, M = 1 μg/cm^2, R = 80 kΩ; and (c) #8, M = 10 μg/cm^2, R = 7 kΩ. (d) Cross-section of the scratched area in sample c.

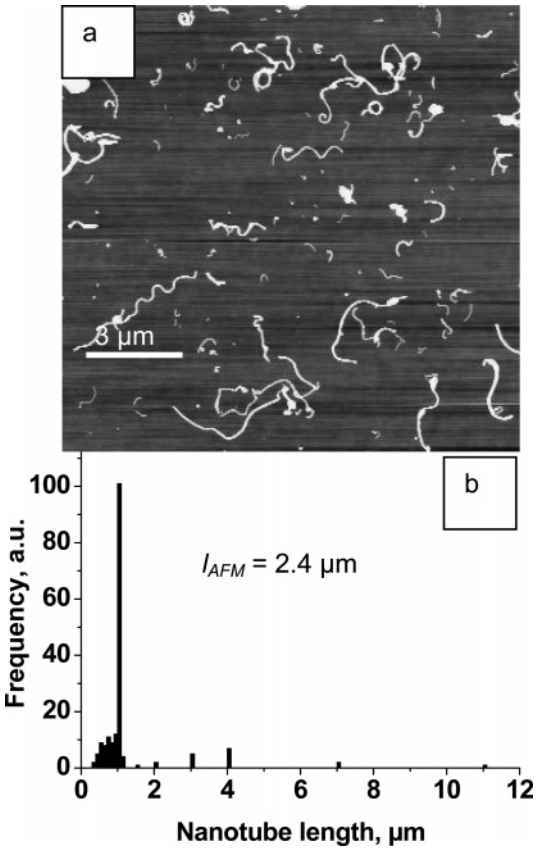

Figure 4. AFM topography image of the CNT-*g*-P2VP (a); distribution of the contour length of the CNT-*g*-P2VP nanotubes (b).

critical exponent.[20] The best fit of the experimental data is observed with $1/R\square^0$ = 50 (1/kOhm per sq) and α = 1.24. The value of the critical exponent, α, is only slightly lower than the value predicted by the percolation theory for 2D-films ($\alpha \sim$ 1.3). Similar deviations of the critical exponent from the theoretical value have been previously observed for CNT-containing composites and accounted for by the very high aspect ratio of the filler. Whenever it is so, the percolation process is not actually statistical, it deviates from the random distribution of these too long individual objects.[6,24,25]

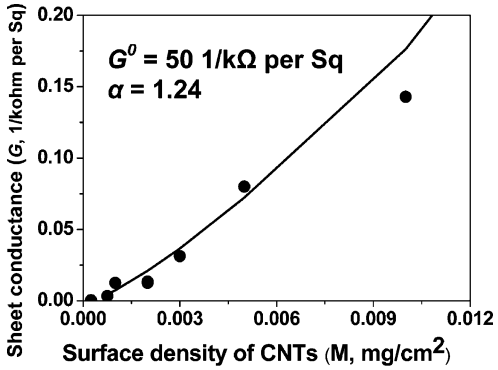

Figure 5. Sheet conductance vs surface density of the CNT-*g*-P2VP. The experimental data in the percolation region were fitted with a critical exponent $\alpha = 1.24$.

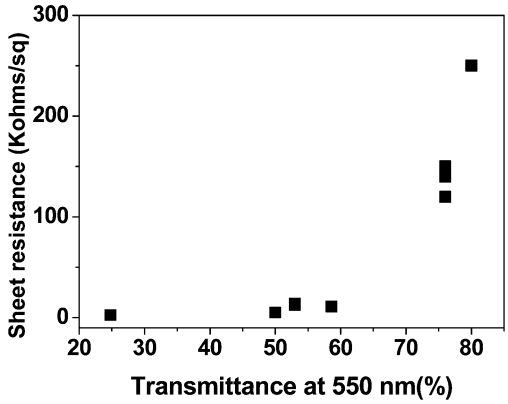

Figure 6. Transmittance at 550 nm for CNT-*g*-P2VP films of different sheet resistances.

The transmittance, *T*, of the CNT-*g*-P2VP films with different surface densities has been measured for samples cast on glass slides. Figure 6 shows how *T* at 550 nm changes with the sheet resistance *R*□. *R*□ is in the range of 20−50 kΩ whenever *T* does not exceed 70. Beyond this *T* value, *R*□ increases sharply.

The CNT-*g*-P2VPs nanotubes have also been dispersed in THF, and a series of films of various thicknesses have been prepared. As a rule, the films are less homogeneous as seen by the naked eye and the sheet resistance is approximately 2 orders of magnitude higher compared to the counterparts prepared from acidic aqueous dispersions.

3. Discussion and Conclusions

Deposition of CNT-*g*-P2VP from aqueous dispersions at low pH is an effective method to prepare ultrathin films with a tunable CNTs density. A percolation threshold of 0.25 μg/cm^2 and a critical exponent $\alpha = 1.24$ have been found from dc conductivity measurements. The □ value agrees with the percolation theory for 2D films. According to AFM and electrical measurements, even when only 5% of the surface is covered by CNT-*g*-P2VPs, the sheet resistance is of the order of 1 MΩ/sq, which indicates that conductivity is imparted by a network of an ultralow density. When the film transmittance decreases down to ∼70% at 550 nm, the occupied surface area is ∼15% and *R*□ falls down to ∼90 kΩ/sq. These data show that undesired in-plane clustering does not occur upon the dispersion casting of the films and that high-quality networks of CNT-*g*-P2VPs are built up. The electrosteric stabilization of the CNT-*g*-P2VP dispersions in water at low pH is at the origin of this desired behavior.

4. Experimental Section

Commercially available CNTs (MWNT THICK, Nanocyl S. A., Belgium, 50 μm long, average inner diameter 6 nm, outer diameter 25 nm, and purity higher than 95 wt %) were used without further purification. They were modified by grafting of P2VP chains ($M_n = 7606$; $M_w/M_n = 1.37$) as previously reported[17] and dispersed in acidic water (pH 2). Si-wafers with an insulating SiO_2 layer of about 300 nm (from Wacker-Chemitronics) and glass slides (Menzel-Glaser) were repeatedly cleaned (at least 3 times) in a ultrasonic bath with dichloromethane (DCM) for 5 min, and then treated with a cleaning solution of NH_4OH and H_2O_2 at 60 °C for 1 h.

CNT-*g*-P2VP Films. Freshly cleaned Si-wafers (or glass slides) were placed onto a heating stage at 150 °C. One drop of the CNT-*g*-P2VP dispersion of well-defined volume and concentration (Table 1) was deposited on the surface. After evaporation of water (within few seconds), the samples were characterized by several techniques.

AFM Measurements. The Multimode AFM instrument (Digital Instruments, Santa Barbara) was operated in the tapping mode. Silicon tips with a 10−20 nm radius, a spring constant of 30 N/m, and a resonance frequency of 250−300 kHz were used.

UV−Vis Measurements. These measurements were carried out with a Perkin-Elmer UV/vis Spectrometer Lambda 19.

Ellipsometry. Ellipsometric measurements were carried out on a rotating-analyzer (RA) ellipsometer SE400 (SENTECH Instruments GmbH, Germany). The instrument uses a He−Ne laser as a light source ($\lambda = 632.8$ nm) and is equipped with focusing optics collimating a laser beam in a 30 μm size spot on sample surface and a XY-stage for mapping measurements. The incident angle was fixed at 70°. The thickness of the graphite constituting the given MWNTs film was calculated by using a three-layer model: $Si-SiO_2$/graphite/air. The ellipsometric parameters were fitted by using the Elli program developed by Optrel GBRmBH (thickness of $SiO_2 = 149 \pm 1.5$ nm; $n_{SiO_2} = 1.4598$; $n_{Si} = (3.858 - i0.018)$; $n_{air} = 1$; $n_{graphite} = 2.10 - i(0.6-0.8)$ (was fixed)).

Electrical Measurements. Two electrodes (1 cm in width) were covered by alumina foil and fixed on the sample surface with an interdistance of 0.5 cm. dc-electrical measurements were performed with a Keithley 236 Source-Measure Unit. At least 10 electrical measurements were undertaken for each sample.

Acknowledgment. Financial support was provided by the European Scientific Foundation (ESF), the Deutsche Forschungsgemeinschaft (DFG), and the Belgian "Fonds National de la Recherche Scientifique" (FNRS) within the ESF EUROCORES/SONS program (02-PE-SONS-092-NEDSPE). X.L., F.S., R.J., and C.D are much indebted to the "Région Wallonne" for support in the frame of the "Nanotechnologies" program ENABLE and to the "Belgian Science Policy" for financial support in the frame of the "Interuniversity Attraction Poles Programme (PAI V/03)". C.D. is Chercheur Qualifié by the FNRS, which also provided F.S. with a fellowship. We thank Dr. Klaus-Jochen Eichhorn for the helpful discussion of the ellipsometric data.

References and Notes

(1) Dresselhaus, M. S.; Dresselhaus, G.; Avouris, P. *Carbon Nanotubes*: *Synthesis, structure, Properties, and Applications*; Springer-Verlag: New York, 2001. Dai, H. *Acc. Chem. Res.* **2002**, *35*, 1035.

(2) Raravikar, N. R.; Vijayaraghavan, A. S.; Keblinski, P.; Schadler, L. S.; Ajayan, P. M. *Small* **2005**, *1*, 317. Koganemaru, A.; Bin, Y.; Agari, Y.; Matsuo, M. *Adv. Funct. Mater.* **2004**, *14*, 842. Barisci, J. N.; Tahhan,

M.; Wallace, G. G.; Badaire, S.; Vaugien, T.; Maugey, M.; Poulin, P. *Adv. Funct. Mater.* **2004**, *14*, 133. Bryning, M. B.; Islam, M. F.; Kikkawa, J. M.; Yodh, A. G. *Adv. Mater.* **2005**, *17*, 1191. Ramasubramaniam, R.; Chen, J.; Liu, H. Y. *Appl. Phys. Lett.* **2003**, *83*, 2928.

(3) Li, S.; Qin, Y.; Shi, J.; Guo, Z.-X.; Li, Y. Zhu, D. *Chem. Mater.* **2005**, *17*, 130. Qu, L.; Lin, Y.; Hill, D. E.; Zhou, B.; Wang, W.; Sun, X.; Kitaygorodskiy, A.; Suarez, M.; Connell, J. W.; Allard, L. F.; Sun, Y.-P. *Macromolecules* **2004**, *37*, 6055.

(4) Grunlan, J. C.; Mehrabi, A. R.; Bannon, M. V.; Bahr, J. L. *Adv. Mater.* **2004**, *16*, 150.

(5) Saran, N.; Parikh, K.; Suh, D.-S.; Munoz, E.; Kolla, H.; Manohar, S. K. *J. Am. Chem. Soc.* **2004**, *126*, 4462.

(6) Gubbels, F.; Blacher, S.; Vanlathem, E.; Jerome, R.; Deltour, R.; Brouers, F.; Teyssie, Ph. *Macromolecules* **1995**, *28* (5), 1559−66. Gubbels, F.; Jerome, R.; Vanlathem, E.; Deltour, R.; Blacher, S.; Brouers, F. *Chem. Mater.* **1998**, *10*, 1227−1235.

(7) Glatkowski, P.; et al., U.S. Patent 6,265,466, July 24, 2001.

(8) Sandler, J.; Shaffer, M. S.; Prasse, P. T.; Bauhofer, W.; Schulte, K.; Windle, A. H. *Polymer* **1999**, *40*, 5967. Smith, J. G.; Connel, J. W.; Delozier, D. M.; Lillehei, P. T.; Watson, K. A.; Lin, Y.; Zhou, B.; Sun Y. P. *Polymer* **2004**, *45*, 825.

(9) Kuttel, O.; Groening, O.; Emmenegger, C.; Schlapbach, L. *Appl. Phys.Lett.* **1998**, *73*, 2113. Lim, S.; Jeong, H.; Park, Y.; Bae, D.; Choi, Y.; Shin, Y.; Kim, W.; An, K.; Lee, Y. J. *Vac. Sci. Technol. A* **2001**, *19*, 1786.

(10) Park, J.-U.; Meitl, M. A.; Hur, S.-H.; Usrey, M. L.; Strano, M. S.; Kenis, P. J. A.; Rogers, J. A. *Angew. Chem., Int. Ed.* **2006**, 45, 581. Panhuis, M.; Gowrisanker, S.; Vanesko, D. J.; Mire, C. A.; Jia, H.; Xie, H.; Baughman, R. H.; Musselman, I. H.; Gnade, B. E.; Dieckmann, G. R.; Draper, R. K. *Small* **2005**, *1*, 820. Hirsch, A. *Angew. Chem., Int. Ed.* **2002**, *41*, 1853. Star, A.; Steuermann, D. J.; Heath, R.; Stoddard, J. F. *Angew. Chem., Int. Ed.* **2002**, *41*, 2508. Petrov, P.; Stassin, F.; Pagnoulle, C.; Jerome R. *Chem. Commun.* **2003**, 2904. Niyogi, S.; Hamon, M. A.; Hu, H.; Zhao, B.; Bhowmik, P.; Sen, R.; Itkis, M. E.; Haddon, R. C. *Acc. Chem. Res.* **2002**, *35*, 1105. Sun, Y.-P.; Fu, K.; Lin, Y.; Huang, W. *Acc. Chem. Res.* **2002**, *35*, 1096. Viswanathan, G.; Chakrapani, N.; Yang, H.; Wei, B.; Chung, H.; Cho, K.; Ryu, C. Y.; Ajayan, P. M. *J. Am. Chem. Soc.* **2003**, *125*, 9258. Yao, Z.; Braidy, N.; Botton, G. A.; Adronov, A. *J. Am. Chem. Soc.* **2003**, *125*, 16015. Qin, S.; Qin, D.; Ford, W. T.; Resasco, D. E.; Herrera, J. E. *J. Am. Chem. Soc.* **2004**, *126*, 170. Kong, H.; Gao, C.; Yan, D. *J. Am. Chem. Soc.* **2004**, *126*, 412. Qin, S.; Qin, D.; Ford, W. T.; Resasco, D. E.; Herrera J. E. *Macromolecules* **2004**, *37*, 752. Sabba, Y.; Thomas, E. L. *Macromolecules* **2004**, *37*, 4815. Fernando, K. A. S.; Lin, Y.; Sun, Y.-P. *Langmuir* **2004**, *20*, 4777. Sinani, V. A.; Gheith, M. K.; Yaroslavov, A. A.; Rakhnyanskaya, A. A.; Sun, K.; Mamedov, A. A.; Wicksted, J. P.; Kotov, N. A. *J. Am. Chem. Soc.* **2005**, *127*, 3463.

(11) Sreekumar, T. V.; Liu, T.; Kumar, S.; Ericson, L. M.; Hauge, R. H.; Smalley, R. E. *Chem. Mater.* **2003**, *15*, 175.

(12) Hu, L.; Hecht, D. S.; Gruner G. *Nano Lett.* **2004**, *4*, 2513.

(13) Wu, Z.; Chen, Z.; Du, X.; Logan, J.; Sippel, J.; Nikolou, M.; Kamaras, K.; Reynolds, J.; Tanner, D.; Hebard, A.; Rinzler, A. *Science* **2004**, *305*, 1273.

(14) Meitl, M. A.; Zhou, Y.; Gaur, A.; Jeon, S.; Usrey, M. L.; Strano, M. S.; Rogers, J. A. *Nano Lett.* **2004**, *4*, 1643.

(15) Baughman, R. H.; Zhakhidov, A. A.; de Heer, W. A. *Science* **2002**, *297*, 787.

(16) Simple calculations show that the individual MWNT with the outer and inner diameter of 25 and 6 nm, respectively, contains more carbon atoms with the factor of about 2.2 than the 25-nm-thick bungle of SWNTs with the diameter of 1.5 nm.

(17) Lou, X.; Detrembleur, C.; Pagnoulle, C.; Jérôme, R.; Bocharova, V.; Kiriy, A.; Stamm, M. *Adv. Mater.* **2004**, *16*, 2123.

(18) Vossen, D. L. J.; de Dood, M. J. A.; van Dillen, T.; Zijlstra, T.; van der Drift, E.; Polman, A.; van Blaaderen, A. *Adv. Mater.* **2000**, *12*, 1434.

(19) Tung, J.; Lin, C. *Radiat. Eff.* **1980**, *80*, 261.

(20) Stauffer, G. *Introduction to percolation theory*; Taylor & Francis: London, UK, 1985.

(21) Pike, G. E.; Seager, C. *Phys. Rev. B* **1974**, *10*, 1421. Yi, Y.; Sastry, A. *Phys. Rev. E* **2002**, *66*, 066130. Kirkpatrick, S. *Rev. Mod. Phys.* **1973**, *45*, 574.

(22) WSxM v4.0 Develop 8.1: http://www.nanotec.es/.

(23) The value of the surface density for sample #1 was used as the critical density ($M_{\#1} = M_C$) since the calculated density of conductive sticks for this sample ($N_{\#1} = 1.06\ 1/\mu m^2$) is very close to the calculated critical density ($N_C = 0.99\ 1/\mu m^2$).

(24) Kim, B.; Lee, J.; Yu, I. *J. Appl. Phys.* **2003**, *94*, 6724.

(25) Kilbride, B. E.; Coleman, J. N.; Fraysee, J.; Fournet, P.; Cadek, M.; Drury, A.; Hutzler, S.; Roth, S.; Blau, W. J. *J. Appl. Phys.* **2002**, *92*, 4024.